Ambient particulate matter attenuates Sirtuin1 and augments SREBP1-PIR axis to induce human pulmonary fibroblast inflammation: molecular mechanism of microenvironment associated with COPD

Chia-Ping Tien[1,2,3], Chia-Hung Chen[4], Wen-Yuan Lin[2,5,6], Chiu-Shong Liu[2,5,6], Ko-Jiunn Liu[7], Michael Hsiao[3,8], Yu-Chan Chang[3], Shih-Chieh Hung[9,10,11]

[1]Ph.D. Program for Aging, College of Medicine, China Medical University, Taichung, Taiwan
[2]Division of Community and Family Medicine, China Medical University Hospital, Taichung, Taiwan
[3]Genomics Research Center, Academia Sinica, Taipei, Taiwan
[4]Pulmonary Medicine, China Medical University Hospital, Taichung, Taiwan
[5]Department of Social Medicine, College of Medicine, China Medical University, Taichung, Taiwan
[6]Department of Family Medicine, College of Medicine, China Medical University, Taichung, Taiwan
[7]National Institute of Cancer Research, National Health Research Institutes, Tainan, Taiwan
[8]Department of Biochemistry, College of Medicine, Kaohsiung Medical University, Kaohsiung, Taiwan
[9]Drug Development Center, Institute of New Drug Development, China Medical University, Taichung, Taiwan
[10]Integrative Stem Cell Center, China Medical University Hospital, Taichung, Taiwan
[11]Institute of Biomedical Sciences, Academia Sinica, Taipei, Taiwan

Correspondence to: Shih-Chieh Hung, Yu-Chan Chang; email: hung3340@gmail.com, jameskobe0@gmail.com

ABSTRACT

Evidences have shown a strong link between particulate matter (PM) and increased risk in human mortality and morbidity, including asthma, chronic obstructive pulmonary disease (COPD), respiratory infection, and lung cancer. However, the underlying toxicologic mechanisms remain largely unknown. Utilizing PM-treated human pulmonary fibroblasts (HPF) models, we analyzed gene expression microarray data and Ingenuity Pathway Analysis (IPA) to identify that the transcription factor *sterol regulatory element-binding protein 1 (SREBP1)* was the main downstream regulator of *Sirtuin1* (*SIRT1*). Quantitative PCR and western blot results showed that SIRT1 inhibited SREBP1 and further downregulated Pirin (PIR) and Nod-like receptor protein 3 (NLRP3) inflammasome after PM exposure. Inhibitors of SIRT1, SREBP1, and PIR could reverse PM-induced inflammation. An *in silico* analysis revealed that PIR correlated with smoke exposure and early COPD. Immunohistochemical analysis of tissue microarrays from PM-fed mouse models was used to determine the association of PIR with PM. These data demonstrate that the SIRT1-SREBP1-PIR/ NLRP3 inflammasome axis may be associated with PM-induced adverse health issues. SIRT1 functions as a protector from PM exposure, whereas PIR acts as a predictor of PM-induced pulmonary disease. The SIRT1-SREBP1-PIR/ NLRP3 inflammasome axis may present several potential therapeutic targets for PM-related adverse health events.

INTRODUCTION

Epidemiologic studies have suggested a strong link between air pollution and increased risk in human mortality and morbidity, including asthma, chronic obstructive pulmonary disease (COPD), pulmonary infection, and lung cancer. Meanwhile, air pollutants can lead to serious health consequences including stroke, Alzheimer's disease, heart disease, and diabetes. Children, pregnant women, and the elderly are especially vulnerable [1–3]. World Health Organization (WHO) recognizes that fine particles in polluted air is an invisible killer responsible for around 7 million global deaths per year, including 43% from chronic obstructive pulmonary disease, 29% from lung cancer, 25% from heart diseases, 24% from stroke, and 24% from acute lower respiratory infection [1, 4].

The sources of air pollution include industry and energy supply, transport, waste management, dust, agricultural practices, and household energy [3, 5]. Ambient particulate matter (PM) is defined as airborne particles, a mixture of mixtures solid and liquid droplets, composed of alkanes, carbons, aromatic acids, sulfate, nitrate, and ions [6]. Although the underlying toxicologic mechanisms by which PM induces adverse health events remain to be elucidated, it is believed that it is due to its unique characteristics, small size, large surface area, and ability to absorb a large amount of harmful molecules [3]. PM is also considered as a potent oxidants and capable of directly generating reactive oxygen species (ROS), followed by cellular oxidative stress. Oxidative stress can activate redox-sensitive signaling pathways that lead to different biological cascades, including inflammation, DNA damage, and cell death [7]. Additionally, inflammasomes, consist of caspase-1, apoptosis-associated speck-like protein containing a CARD (ASC) and Nod-like receptor protein 3 (NLRP3), imply a wide variety of chronic or acute inflammations, including lung disease [8, 9]. NLRP3 inflammasome activates caspase-1, cleaving the precursor IL-1β and IL-18 into bioactive cytokines, which trigger further inflammatory cascade [8]. Several studies indicate that inflammasomes play a key role in PM-induced lung disease, central nervous system toxicity, cardiovascular disease, reproductive disorders, and skin injury [8, 10–13]. PM, when inhaled, easily bypasses the complete respiratory airway, penetrates alveoli and crosses the air-blood barrier, leading to increased risk in human mortality, morbidity, and hospitalizations, especially in COPD [1–3, 14]. In the current study, we sought to define the role of the inflammasome complex and its subsets in the pathogenesis of PM-related health problems.

It was estimated that COPD, a progressive life-threatening lung disease, caused more than 3 million global deaths in 2012 [15]. Major risk factors of COPD include tobacco smoke, air pollution, occupational dust, chemicals, and respiratory infections [15, 16]. COPD should be suspected in any patient with symptoms of chronic cough, sputum, shortness of breath, and/or history of exposure to noxious stimuli. Global Initiative for Chronic Obstructive Lung Disease (GOLD) guidelines for COPD state diagnosis are established by spirometry with a post-bronchodilator forced expiratory volume in one second (FEV_1) / forced vital capacity (FVC) < 0.70, consistent with the presence of irreversible and progressive airflow limitation [15]. COPD can develop adverse sequelae, including pneumonia, lung cancer, polycythemia, hypertension, cor pulmonale, osteoporosis, skeletal muscle dys-function, weight issues, sleep apnea, diabetes, depression, and anxiety [15].

In the current study, we hypothesized that the inflammation and tissue remodeling mediated by PM may arise from an alternation of gene expression or signaling pathways via inflammasomes, developing respiratory disease. We established transcriptomics data by microarray chips in human pulmonary fibroblasts (HPF), a central player in the fibrosis and airway remodeling of COPD [9], after exposure to PM. Our results confirmed that sterol regulatory element-binding protein 1 (SREBP1) and its downstream target Pirin (PIR) were activated by PM, which could be counteracted by Sirtuin1 (SIRT1). Moreover, we provided evidence that SREBP1 is directly inhibited by SIRT1, and increases expression of inflammasome-related markers in PM-treated HPF cell models [17]. In addition, *in silico* analysis predicted that PIR played a key role in early COPD events. Taking all results into account, therapeutic targeting of SIRT1-SREBP1-PIR/NLRP3-inflammasome axis may be a novel approach against PM-induced fibrosis and inflammation in the human respiratory system.

RESULTS

SREBP1 acts as the activated transcription factor upon PM treatment in HPF

To determine the exact canonical pathways or networking induced by PM in the human respiratory system, we evaluated transcriptomics datasets by microarray chips in HPF (Human Pulmonary Fibroblast) under several PM groups (sham, low dose for 6 hours, low dose for 24 hours, high dose for 6 hours, high dose for 24 hours, low dose = 5 μM, high dose = 50 μM) (Figure 1A). Through Genespring software normalization, 732 genes were found to have > 1.5-fold differential expression in low for 6 hours, low for 24 hours, high for 6 hours, or high for 24 hours relative to

sham in HPF (Supplementary Table 1). The top ranking of candidate genes is shown in Figure 1B. The normalized microarray data was analyzed using IPA to identify significant molecular that are activated in response to PM exposure in HPF. The results showed that the transcription factor *SREBP1* was the No. 1 putative candidates to be activated in response to PM exposure, with the transcriptional activity of its downstream genes of $P = 7.9E-06$ in HPF. The top 7 transcription factors in HPF are shown in Figure 1C. There are 2 *SREBP* genes in mammals, *SREBP1* and *SREBP2*, encoding 3 sterol regulatory element-binding proteins (SREBPs), SREBP-1a, -1c and -2 [18]. *SREBP-1a* acts as a potent activator of all SREBP-responsive genes, stimulating cholesterol, fatty acids, and triglycerides synthesis. SREBP-1c is the main regulator of fatty acid, whereas SREBP-2 is the main regulator of cholesterol [18]. We sought to study if *SREBP1* acts as transcription factors in response to PM, and our quantitative RT-PCR analysis result showed that *SREBP1* was consistent with microarray in HPF (Figure 2A). *SREBP1* was significantly increased in a dose-dependent manner after PM for 6 hours and in a time-dependent manner after PM at low dose. We uploaded our microarray datasets into the SREBP1-related signature from IPA tool, and our analysis showed that *C-X-C motif chemokine ligand 8 (CXCL8), interleukin 6 (IL-6), Pirin (PIR), Interleukin 6 Family Cytokine (LIF), and Interleukin 24 (IL-24)* were the most significantly upregulated transcriptional targets of *SREBP1* (Figure 2B).

SREBP1 activated PIR in response to PM exposure

We further examined the levels of *SREBP1* and its downstream targets, *CXCL8, IL-6, PIR, LIF,* and *IL-24* in the PM treatment groups (sham, low for 6 hours, low for 24 hours, high for 6 hours, high for 24 hours) of HPF. Our quantitative RT-PCR analysis results first showed that *IL-6* and *PIR* were consistent with microarray in HPF, whereas *CXCL8, LIF,* and *IL-24* were not consistent (Figure 2C). Second, response of *PIR, IL-24,* and *LIF* to PM was in a time- and dose-dependent manner. Response of *CXCL8* to PM was found to be in a dose-dependent manner and only in a time-dependent manner at low dose. Response of *IL-6* to PM was only in a dose-dependent manner for 6 hours and only in a time-dependent manner at low dose. Therefore, we assessed the expression of PIR and IL-6 at the protein level in response to PM treatment.

Our western blot results in the PM treatment groups (sham, low for 6 hours, low for 24 hours, high for 6 hours, high for 24 hours) of HPF showed that PIR were significantly overexpressed after exposure to PM. PIR

was significantly increased in a dose-dependent manner for 6 hours and only in a time-dependent manner at low dose (Figure 3A). At present, SREBP1 is a well-established negative target of SIRT1 [17, 19]. We further hypothesize that PIR is negatively associated with SIRT1.

Increased PIR level and activity in cell culture supernatant are significantly correlated with PM exposure

PIR has been identified to possess enzymatic activity [20]. Moreover, delocalization of PIR was identified in melanomas [20]. To address the role of delocalization of PIR, PIR levels and PIR activity in cell culture supernatant of PM-induced models were determined. Our analysis showed that PIR enzymatic activity was significantly overexpressed after high-dose PM exposure (Figure 3B). Furthermore, we examined levels of SREBP1, SIRT1, and PIR in cell culture supernatant. Our result showed that SREBP1 and PIR were significantly increased in a dose-dependent manner, while SIRT1 was significantly suppressed in a dose-dependent manner after PM exposure, which was consistent with our hypothesis that PM exposure can activate the SREBP1-PIR axis via SIRT1 suppression (Figure 3C).

PM exposure can activate the SREBP1-PIR axis, which could be suppressed by SIRT1

In order to validate that PM exposure can activate the SREBP1-PIR axis, which could be suppressed by SIRT1, we administrated the SIRT1 inhibitor Ex527 [21], SREBP1 inhibitor PF429242 [22], and PIR inhibitor TPh A [23] in PM-treated HPF models. First, we administered PF429242 (1 and 10 μM) to PM-treated HPF models, and mRNA level of *SREBP1* was significantly decreased as expected (Figure 3D). The mRNA level of *PIR* was significantly decreased in a dose-dependent manner in response to PF429242 in PM-treated HPF models (Figure 3E). We further examined cell culture supernatant in PF429242-PM co-treated models, and our analysis showed that PIR activity was significantly inhibited by PF429242 in a dose-dependent manner (Figure 3F). These results support the hypothesis that the SREBP1-PIR axis was activated by PM. Second, we administered TPh A (10 and 100 μM) to PM-treated HPF models, and protein levels of PIR were significantly decreased as expected (Figure 3G). Strikingly, the expression of SIRT1 was correlated with the expression of PIR on the protein levels in TPh A-PM co-treated HPF models (Figure 3G). We further examined the cell culture supernatant in TPh A-PM co-treated models, and our analysis
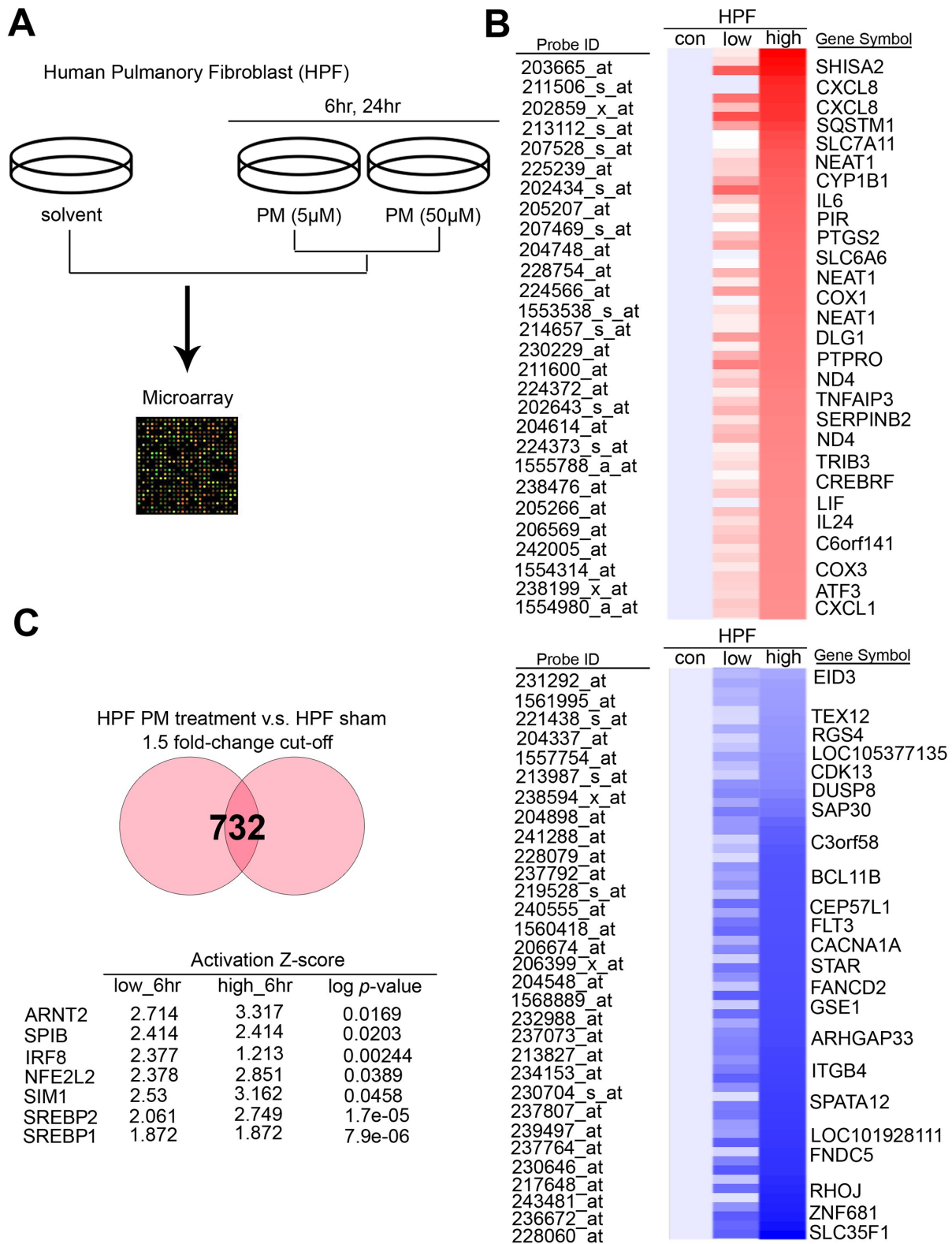
Figure 1. PM induced several potential transcription factors in a dose-dependent manner in normal lung cells. (**A**) The flowchart represents the procedure of microarray chips established in human pulmonary fibroblasts. (**B**) Detailed heatmaps highlight the significantly up- and down-regulated genes after PM treatment, that were normalized gene expression from the microarray database analysis. (**C**) The ranking of candidate transcription factors by IPA database of microarray from PM treatment compared with the sham group in human pulmonary fibroblasts. The cut-off was a 1.5-fold change.
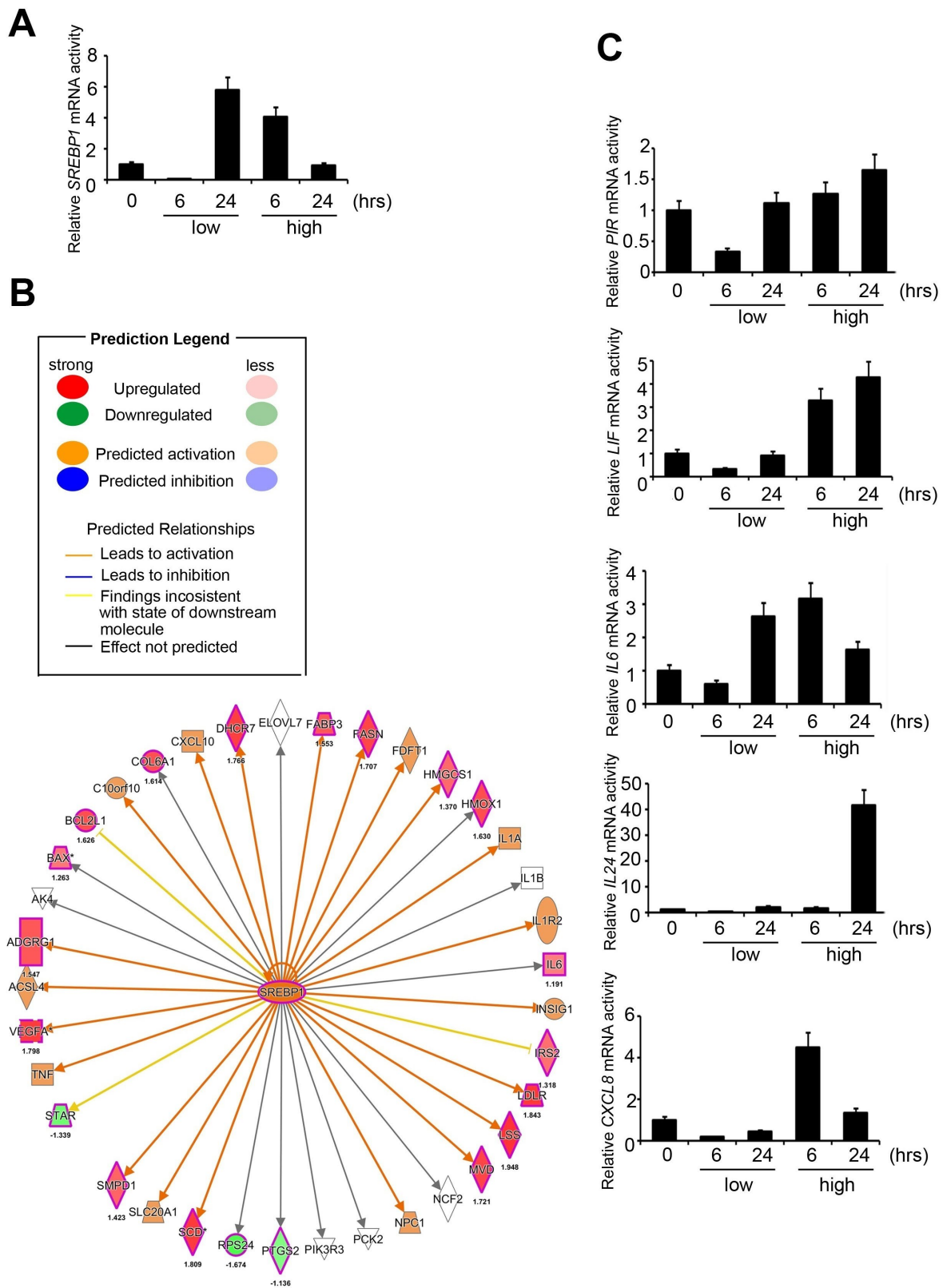
Figure 2. Signatures regulated by PM in HPF models. (**A**) The mRNA level of *SREBP1* after PM treatment. (**B**) The prediction of *SREBP1*-network derived from the common signature, by comparison of IPA database with microarray data from HPF cells with a 1.5-fold-change cut-off. The intensity of the node color indicates the degree of activating (orange) or inhibiting (blue) regulation following PM interaction. (**C**) Several mRNA levels of *SREBP1* downstream factors, including *PIR, LIF, IL-6, IL-24,* and *CXCL8,* after PM treatment in HPF.
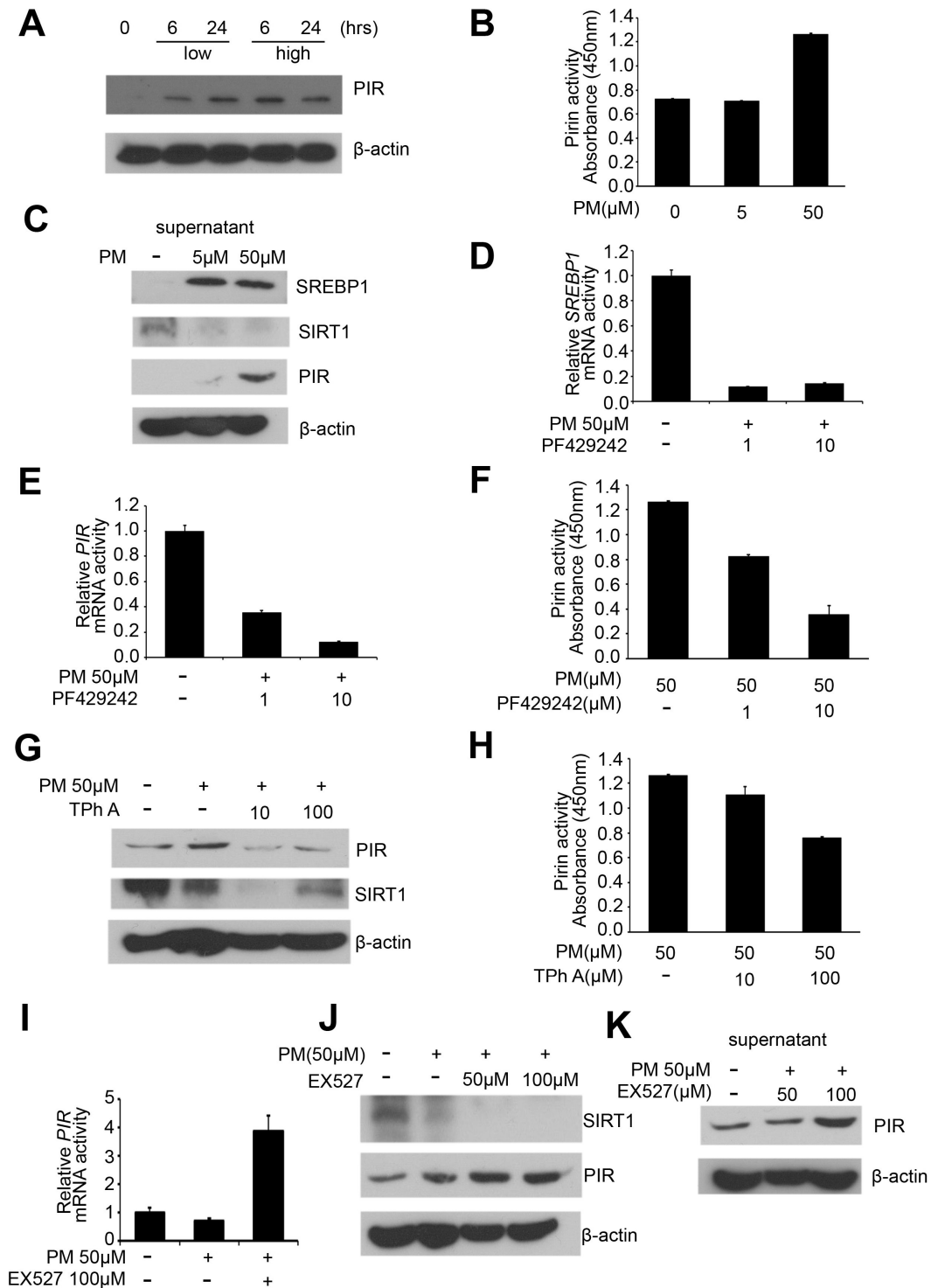
Figure 3. PM exposure is positively correlated with activation of the SREBP1-PIR signaling pathway through SIRT1 downregulation. (**A**) Western blot analysis of PIR after PM treatment in HPF. (**B**) PIR activity from cell culture supernatant in PM-induced models. (**C**) Levels of SREBP1, SIRT1, and PIR were measured from cell culture supernatant of PM-induced models. (**D**) mRNA levels of *SREBP1* in PF429242-PM co-treated HPF models. (**E**) mRNA levels of *PIR* in PF429242-PM co-treated HPF models. (**F**) PIR activity from cell culture supernatant in PF429242-PM co-treated HPF models. (**G**) Western blot analysis of PIR and SIRT1 in TPh A-PM co-treated HPF models. (**H**) PIR activity from cell culture supernatant in TPh A-PM co-treated HPF models. (**I**) mRNA level of *PIR* in Ex527-PM co-treated HPF models. (**J**) Western blot analysis of SIRT1 and PIR in Ex527-PM co-treated HPF models. (**K**) Level of PIR was measured from cell culture supernatant in Ex527-PM co-treated HPF models.

showed that PIR activity was significantly inhibited in a dose-dependent manner as expected (Figure 3H). Third, we administered Ex527 (100 μM) to PM-treated HPF models, and our quantitative RT-PCR analysis showed that *PIR* was significantly overexpressed (Figure 3I). Afterwards, we further performed western blot analysis. We found Ex527 (50 and 100 μM) suppressed the expression of SIRT1 as expected, while Ex527 increased the expression of PIR in a dose-dependent manner (Figure 3J). Our analysis further showed that PIR in cell culture supernatant was significantly increased in a time- and dose-dependent manner in Ex527-PM co-treated models, which was consistent with expression on PIR protein level (Figure 3J, 3K).

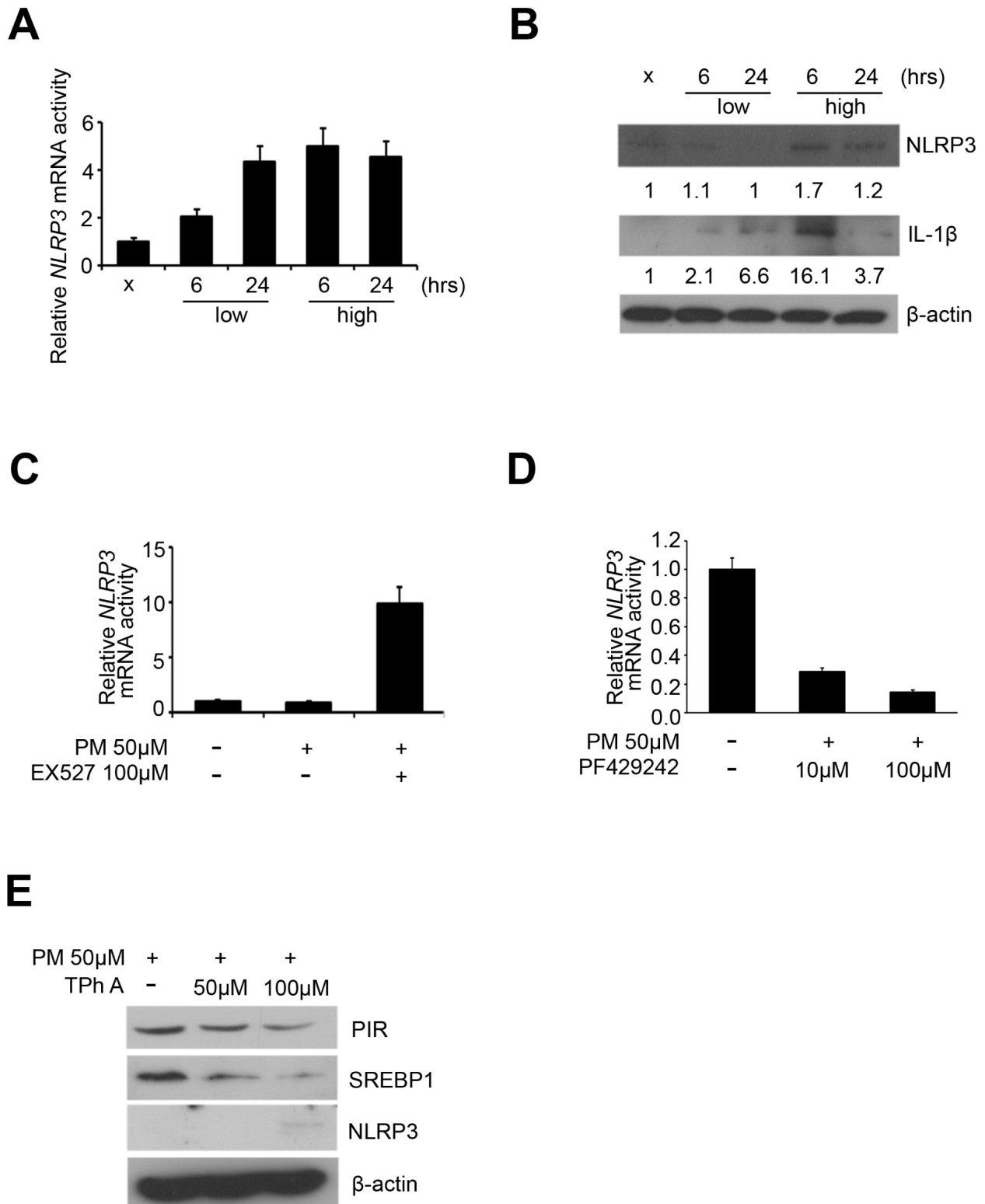## NLRP3 inflammasome may be activated by PM exposure via SREBP1-PIR axis

Previous studies have identified that the protein complex called inflammasomes, play a central role in the acute lung injury and chronic pulmonary diseases [8]. NLRP3 and IL-1β were considered as characteristic markers of inflammasomes [8]. We first carried out quantitative RT-PCR analysis to detect the expression of *NLRP3* in the 5 PM treatment groups (sham, low for 6 hours, low for 24 hours, high for 6 hours, high for 24 hours) of HPF, and our results showed that *NLRP3* was overexpressed in dose-dependent manner in response to PM and only in a time-dependent manner at low dose (Figure 4A). We further carried out western blot to detect the expression of IL-1β and NLRP3 in the 5 PM treatment groups of HPF. After normalized against β-actin and quantified via ImageJ, NLRP3 was overexpressed in a dose-dependent manner for both 6 and 24 hours, while IL-1β was overexpressed in a dose-dependent manner for 6 hours and in a time-dependent manner at low dose (Figure 4B). Previous studies indicate that SREBP1, directly deacetylated and inhibited by SIRT1, increases expression of inflammasomes [17]. Thus, we hypothesized that exposure to PM suggests induction of the SREBP1-NLRP3 inflammasome pathway, via SIRT1 inhibition. We further validated the mRNA expression of *NLRP3* in Ex527-PM and PF429242-PM co-treated HPF models. By quantitative RT-PCR analysis, Ex527 significantly upregulated *NLPR3*, while PF429242 significantly inhibited *NLRP3* in a dose-dependent manner (Figure 4C, 4D). In TPh A-PM co-treated HPF models, the expression of PIR and SREBP1 were both downregulated in a dose-dependent manner, while NLRP3 was upregulated in a dose-dependent manner (Figure 4E).

PIR acts as a biomarker for detecting early COPD

To determine the clinical association between PIR and PM, we verified several previously developed micro-

array databases to identify and compare the correlation between *PIR* and nonsmokers, smokers, early COPD, and COPD using the Gene Expression Omnibus (GEO) databases. By analyzing a microarray cohort collecting small airway epithelium from phenotypically normal smokers and non-smokers, relative to nonsmokers, *PIR* was found to be the most activated gene to have a significant correlation with smoking (Figure 5A-5B, *P* < 0.0001) (GSE4498, n = 22). An *in vitro* study, assessing human airway epithelial cells, identified that air pollution stimulates a time- and dose- dependent increase in mRNA level of *IL-6* via nuclear factor kappa B (NF-κB) mediated ROS [24]. Moreover, a multicenter longitudinal study that assessed 955 myocardial infarction survivors from six European cities identified a strong correlation between *fibrinogen beta chain (FGB)* and *IL-6* and worse outcome after exposure to air pollutions [25]. Herein, we studied whether smoke exposure could induce genetic expression of *FGB* and *IL-6*. Our analysis showed that *FGB* and *IL-6* had no significant association with smoking (Figure 5B, *P* = 0.0582 and *P* = 0.1572, respectively) (GSE4498, n = 22). In another microarray database comprised of large airway epithelium from phenotypically normal smokers, non-smokers, early COPD, and COPD, *PIR* was found to have a strong correlation with smoking (Figure 5C, GSE5060, n = 38). We further studied whether severity of COPD was correlated with genetic expression of *PIR*, *FGB*, and *IL-6*. Notably, relative to COPD, *PIR* was found to be the most activated gene to have a significant correlation with early COPD (Figure 5C-5D, *P* < 0.0001), followed by *FGB* (Figure 5D, *P* = 0.0006), while *IL-6* had no significant association (Figure 5D, *P* = 0.3742) (GSE5060, n = 38). In order to validate if PIR is far superior in detecting early COPD, we next identified PIR protein expression using our own clinical cohort. By intra-tracheal instillation of PM into lung using mice models, we collected tissue sections from lung to undergo pathologic exam and immunohistochemical examination. The immunohistochemical staining results showed that the PM-treated mice group had higher concentration of the PIR protein in the lung tissue than in the control mice group (Figure 5E).

These data suggested that high PIR protein expression was significantly correlated with PM exposure, which means PIR acts as a predictor of PM-induced cardiopulmonary disease. Together, we identified that PM exposure can activate the SREBP1-PIR/NLRP3 inflammasome signaling pathway, through SIRT1 downregulation (Figure 6A, 6B). The SIRT1-SREBP1-PIR/NLRP3 inflammasome axis may present several potential therapeutic targets for PM-related adverse health consequence.

Figure 4. NLRP3 inflammasome was upregulated by PM exposure. (**A**) mRNA level of *NLRP3* after PM in HPF. (**B**) Western blot analysis of NLRP3 and IL-1β after PM in HPF. (**C**) mRNA level of *NLRP3* in Ex527-PM co-treated HPF models. (**D**) mRNA levels of *NLRP3* in PF429242-PM co-treated HPF models. (**E**) Western blot analysis of PIR, SREBP1, and NLRP3 in TPh A-PM co-treated HPF models.
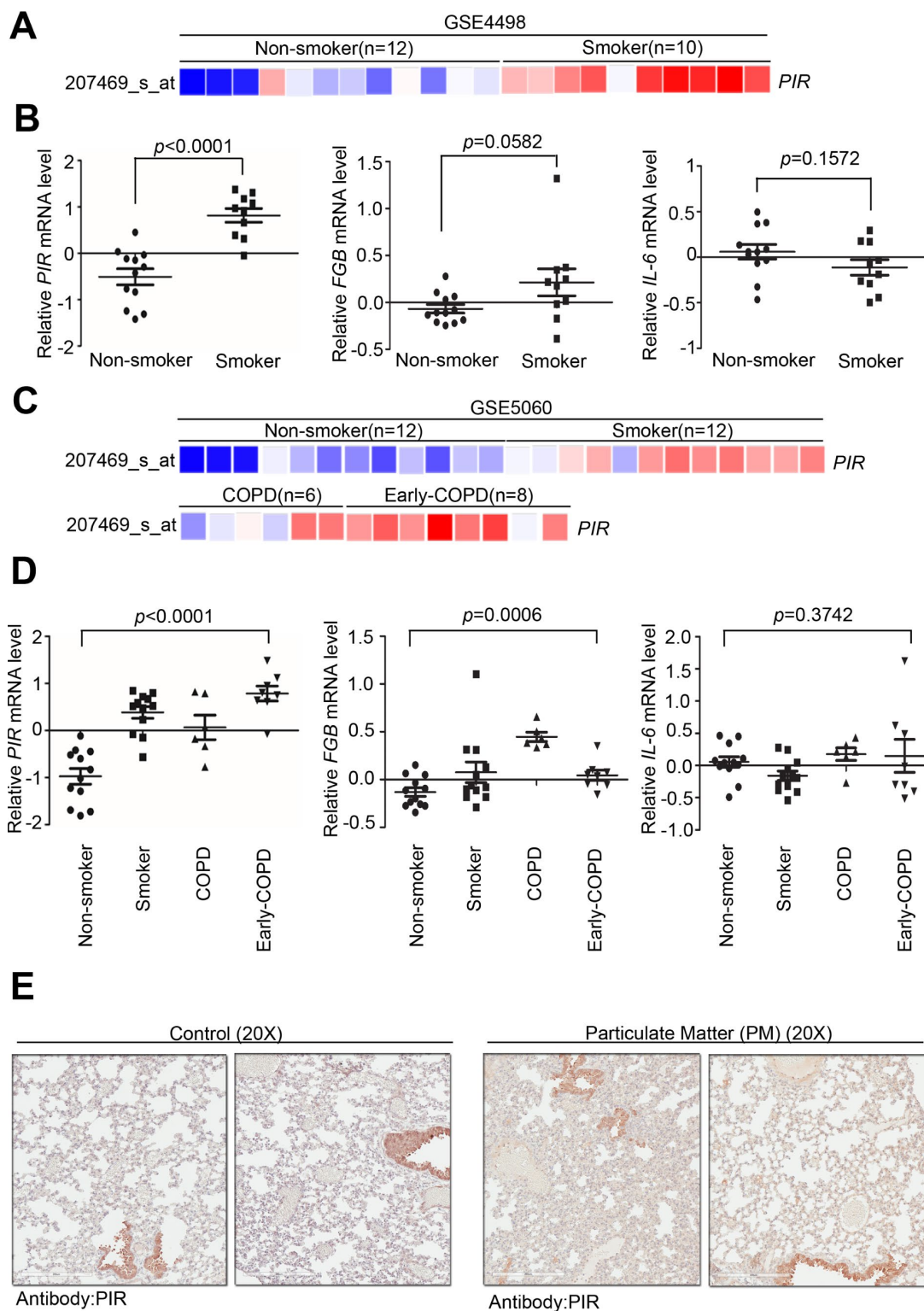
Figure 5. Overexpression of PIR correlates with smoke and early COPD. (**A**) Detailed heatmap highlights the correlation between the mRNA expression level of *PIR* and smoke in the GSE4498 cohort (n = 22) using Oncomine online analysis tool. (**B**) Differential mRNA levels of *PIR*, *FBG*, and *IL-6* between non-smoker and smoker in the GSE4498 cohort. (**C**) Detailed heatmaps highlight the correlation between the mRNA expression levels of *PIR* and non-smoker, smoker, COPD, and early COPD in the GSE5060 cohort (n = 38) using Oncomine online analysis tool. (**D**) Differential mRNA levels of *PIR*, *FBG*, and *IL-6* in non-smoker, smoker, COPD, and early COPD in the GSE5060 cohort. (**E**) The immunohistochemical staining results showed PM-fed mice group had higher concentration of the PIR protein in the lung tissue.
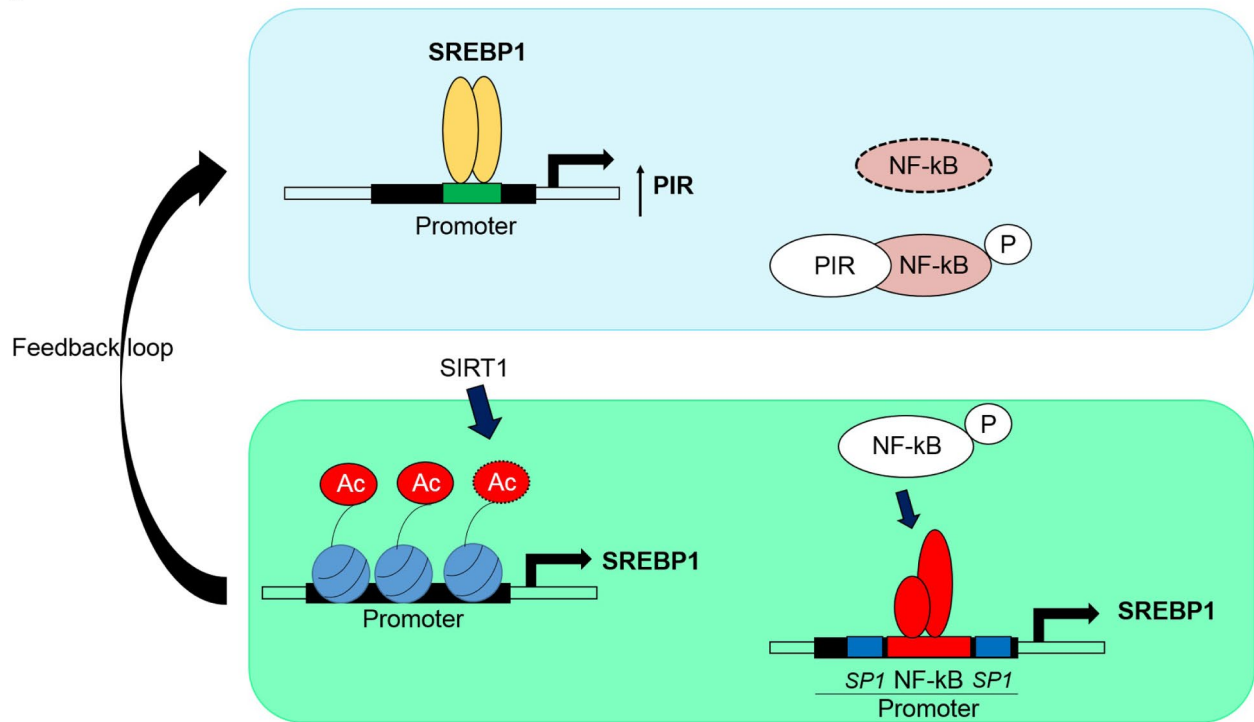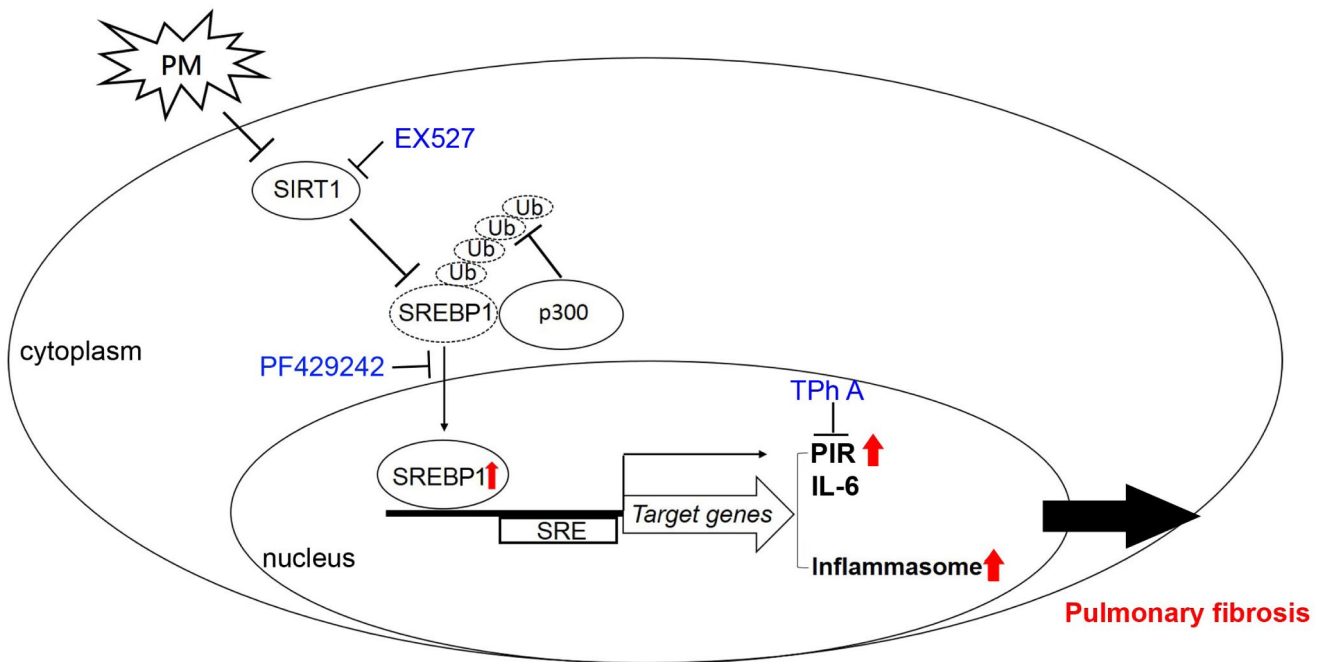
Figure 6. A model illustrates that PM activates the SREBP1-PIR/inflammasomes signaling axis through SIRT1-mediated modulation. (**A**) A schematic model to describe the positive feedback loop and detailed mechanisms of the SIRT1-SREBP1-PIR axis and crosstalk with NF-κB signaling. (**B**) SIRT1 modulates the SREBP1-PIR/NLRP3 inflammasome axis in response to PM. SIRT1 functions as a protector from PM exposure. The SIRT1-SREBP1-PIR/NLRP3 inflammasome axis may present an attractive therapeutic target for PM-related adverse health events.

DISCUSSION

PM exposure is believed to be strongly linked to systemic diseases, majorly cardiopulmonary diseases [1, 4]. Alternate NF-κB redox-regulated signaling pathways have been identified to be a mediator of PM-mediated inflammation and carcinogenesis [26]. PIR, encoded by the *PIR* gene, acts as an iron-dependent redox regulator of NF-κB. PIR is a nuclear protein detectable in all human tissues [27]. Though the function of PIR has not been well studied, it is known to stabilize the formation of quaternary complexes between oncoprotein B-cell lymphoma 3-encoded (Bcl-3), anti-apoptotic protein NF-κB, and its target DNA [28]. Air pollution was identified to activate *IL-6* expression in human airway epithelial cells via NF-κB [24], though in our analysis *IL-6* had no significant association with smoking, whereas PIR was significantly correlated with smoking. PM induces adverse health events via multi-factorial mechanisms (Supplementary Figure 1); therefore, the existence of crosstalk between IL-6 and PIR needs to be addressed. Several intensive researches in the field of cancer show that PIR may act as a relevant role in melanoma and acute myeloid leukemia [23, 29]. A recent *in vitro* study demonstrated that increased expression of PIR was induced by smoke [30], whereas another *in vivo* study on 13 phenotypically normal smokers and 9 non-smokers showed that overexpression of PIR played a role in lung epithelial cell apoptosis in response to cigarette smoke [28]. Surprisingly, we found that PIR could be a biomarker for detecting early COPD. The lack of overexpression of PIR in COPD was surprising because PIR-related apoptosis was thought to result COPD [28]. In contrast to our result however, upregulation of PIR from the human small airway epithelium (n = 33) was consistent with the pathogenesis of COPD [31]. Indeed it was previously documented that tobacco-induced emphysema was independent of NF-κB [32]. Reduction of *PIR* was detected in neonatal mouse respiratory distress disease by cDNA microarray analysis [33]. The plausible explanation is that COPD is a multi-factorial and complex disease, involved in variety of factors and cells [15], the inhibition or inactivation of PIR in each stage of COPD need further elucidated.

Previous *in vitro* and *in vivo* researches suggest that SIRT1 negatively regulates NF-κB-proinflammatory axis in lung disease, including COPD and allergic asthma [34]. Moreover, a recent study demonstrated that SIRT1 functions as a protector from inflammation and coagulation via modulating NF-κB activation following PM exposure [35]. The mechanism of SIRT1 regulation in response to PM, nevertheless, remains to be elucidated. Our data showed that PM inhibited SIRT1 activity, which confirmed the protective role of

SIRT1 in response to PM. A feedback loop between SIRT1 and NF-κB had been documented [36]. SIRT1 mRNA and protein levels as well as SIRT1 promoter activity upregulated in NF-κB overexpression cell models, while SIRT1 protein expression and SIRT1 promoter activity decreased in NF-κB knockdown cell models. Our results revealed that the expression of SIRT1 was correlated with the expression of PIR at the protein levels in TPh A-PM co-treated HPF models (Figure 3G), which supported the hypothesis that SIRT1 may interact with NF-κB inflammation via PIR. Our results further revealed that PM exposure can activate SREBP1-PIR signaling pathway through SIRT1 downregulation. Therefore, SIRT1 may interfere with NF-κB inflammation via the SREBP1-PIR signaling pathway.

In addition to disrupting inflammation, recent studies demonstrated that SIRT1 inhibits NF-κB to suppress various metabolic diseases, including glucose homeostasis and cardiovascular disease [35, 37]. However, the crosstalk controlling metabolism between SIRT1 and NF-κB remains unclear. Several *in vitro* studies revealed that SIRT1-SREBP1 protect mice from hepatic lipogenesis [19, 38]. A study showed that fenofibrate, clinically used to reduce lipid levels, prevented rabbits with atrial fibrillation from atrial metabolic remodeling through the SIRT1-SREBP1 pathway [39]. Another study showed that fenofibrate regulated hyperglycemia-induced metabolic memory via SIRT1-dependent suppression of NF-κB in human retinal endothelial cells [40]. In addition, fenofibrate inhibited the inflammatory response via SIRT1-dependent suppression of NF-κB in adipocytes [41]. On the basis of previous work and this study, SIRT1 may acts as a protector from PM-related consequences, including cardiopulmonary and metabolic disease, by interfering in NF-κB inflam-mation via SREBP1-PIR signaling pathway. Interestingly, both *in vitro* and *in vivo* experiments documented that NF-κB-mediated activation of SREBP1 pathway increased lipid biosynthesis through binding to promoter region [42]. Previously studies have also claimed that PIR acts as a cofactor for NF-κB activity [27], which was consistent with our observation that both the total form and phosphorylation form of NF-κB were inhibited in TPh A-PM co-treated HPF models (Supplementary Figure 2). Our results revealed the expression SREBP1 were downregulated in a dose-dependent manner in TPh A-PM co-treated HPF models (Figure 4E), which supported the positive feedback loop between SREBP1 and NF-κB quaternary complexes (Figure 6A).

Several studies indicate that NLRP3 inflammasome activation played a key role in PM-induced lung disease, mediated by NF-κB [10]. However in our

study, TPh A, reducing the binding affinity between PIR and Bcl3 in NF-κB quaternary complexes, upregulated NLRP3 protein expression in a dose-dependent manner in PM-treated HPF models, which suggested that NLRP3 inflammasome promoted PM-induced adverse health events without dependence on NF-κB quaternary complexes [23]. Furthermore, *in vivo* evidence from translational studies indicated that the dysregulation of SIRT1-SREBP1-NLRP3 inflamma-some may contribute to atherosclerosis [17]. Based on previous evidence and on our results, SIRT1-SREBP1-inflammasomes is another plausible axis in response to PM.

Exposure to PM was responsible for high mortality. Of the number of global deaths in specific disease categories, COPD was attributed as the leading cause of death by air pollution and is already the 3rd leading cause of deaths worldwide [43]. COPD is characterized by predominantly pulmonary infiltration inflammatory cells, including macrophages, neutrophils, and T lymphocytes [15]. These inflammatory cells, together with structure cells, including epithelial and endothelial cells and fibroblasts, release multiple inflammatory mediators, including chemokines, inflammasomes, cytokines, free radicles, lipid mediators, protease, and growth factors, amplifying the inflammatory cascade and triggering airway remodeling [44]. Lung function tests assess the severity of disease in COPD. However, biomarkers have been sought for diagnosis, disease progression, exacerbation risk, and therapeutic response [45]. In 2009, SIN and VESTBO reviewed the current candidate plasma or serum biomarkers linked to COPD and found that the systematic inflammatory mediators most associated with COPD outcomes were fibrinogen and C-reactive protein (CRP) [46]. There have been further conflicting reports in large COPD cohorts [47]. IL-6, leading to a rise in plasma fibri-nogen and CRP, was significantly raised in COPD and elevated during exacerbations in the Evaluation of COPD Longitudinally to Identify Surrogate Endpoints (ECLIPSE) cohort [48]. Conversely, our quantitative RT-PCR results showed that *IL-6* responded only in a dose-dependent manner for 6 hours and in a time-dependent manner at low dose (Figure 2C), while our *in silico* analysis showed that *IL-6* had no significant association with COPD (Figure 5D, P = 0.3742) (GSE5060, n = 38). Ilumets et al. reported that matrix metalloproteinases-9 (MMP-9) in induced sputum and plasma appeared to be overexpressed in smokers [49]. However, in humans, steroid therapy showed no effect on MMP-9 levels [50]. Ilumets et al. also mentioned that MMP-8 in the sputum dis-tinguished individuals with asymptomatic COPD, at risk of developing COPD, from healthy smokers, while Sng et al. reported a negative correlation between MMP-8 with exhaled breath condensate in COPD patients when compared to healthy controls [49, 51]. Several clinical trials demonstrated that higher blood eosinophil counts may present increased exacerbation frequency and predict better medicine response [15]. Ichikawa *et al.* indicated that SIRT1 decreased in lung tissue coupled with inflammatory cell infiltration, eosinophilia, and cytokine production in an asthmatic mouse model [52]. Together, PIR may serve as a sensitive biomarker for early stage cardiopulmonary disease elicited by COPD and a predictor for medicine response. However, the importance and specific role of SIRT1 in modulating eosinophil activity remains unidentified. Additionally, further studies are needed to clarify if PIR could be a biomarker for assessing the outcome of COPD.

In summary, our studies demonstrate that SIRT1 modulates the SREBP1-PIR/NLRP3 inflammasome axis in response to PM, indicating that the SIRT1-SREBP1-PIR/ NLRP3 inflammasome axis may be associated to adverse health issues. SIRT1 functions as a protector from PM exposure, whereas PIR acts as a predictor of PM-induced cardiopulmonary disease. The SIRT1-SREBP1-PIR/ NLRP3 inflammasome axis may present an attractive therapeutic target for PM-related adverse health events.

MATERIALS AND METHODS

PM

We purchased urban dust from Urban dust (1649b, NIST® SRM®, Gaithersburg, MD, USA). The dried PM samples were diluted with sterilized phosphate-buVered saline solution (PBS, pH 7.2) and then frozen at −80 C prior to use.

PM treatment

After reviewing the literature [53], we chose 5 μM PM as low dose and 50 μM as high dose. HPF was incubated with PM 5 μM, 50 μM, or sham for 6 hours and 24 hours. We estimated the global RNA expression for extra 6 hours, which is the optimal time point at which mRNAs and genes are fully transcribed by PM treatments. After PM incubation for 6 or 24 hours, we extracted HPF RNA and performed Affymetrix u133 plus 2.0 cDNA microarrays to detect the global and pre-defined gene and mRNA probe changes at the specific time points.

Cell culture and reagents

Human pulmonary fibroblasts (HPF) were purchased from ScienCell research laboratories (Cat. #3300, ScienCell, Carlsbad, CA, USA). They were grown in

fibroblast medium (FM, Cat. #2301, ScienCell, Carlsbad, CA, USA) and stored at 37 °C and 5% CO2. The medium was supplemented with 2% fetal bovine serum (FBS; Cat. #0010, ScienCell, Carlsbad, CA, USA), 1% growth supplement (FGS; Cat. #2352, ScienCell, Carlsbad, CA, USA) and 1% penicillin/streptomycin solution (P/S; Cat. #0503, ScienCell, Carlsbad, CA, USA).

Reagents and compounds

Reagents used for the *in vitro* culture system include Ex527 (Cat. #E7034, Sigma-Aldrich®, Deisenhofen, Germany), PF429242 (Cat. #3354, Tocris Bioscience, Bristol, UK), TPh A (Cat. #TPh A ab144376, Abcam®, Cambridge, MA, USA), and Human Pirin ELISA Kit (Cat. #MBS280347, MyBioSource, San Diego, CA, USA).

RT-qPCR

Total RNA was extracted using TRIzol reagent (Invitrogen, Carlsbad, CA, USA) according to the manufacturer's instruction. The RNA was quantified by NanoDrop (Thermo Fisher Scientific, Waltham, MA, USA). Reverse transcription PCR (RT-PCR) and nested RT-PCR amplification were performed with a SuperScript III kit (Invitrogen, Carlsbad, CA, USA) according to the manufacturer's instruction. The expression level of *Glyceraldehyde 3-phosphate dehydrogenase (GAPDH)* was predominantly used as an internal standard for RT-PCR. The specific primer sequences are as follows: *SREBP1* forward is 5′–GCAAGGCCATCGACTACA TT-3′ and reverse is 5'-GGTCAGTGTGTCCTCCACCT-3′, *C-X-C motif chemokine ligand 8 (CXCL8)* forward is 5′-ATGACTTCCAAGCTGGCCGTGGCT-3′ and reverse is 5′-TCTCAGCCCTCTTCAAAAACTTCTC-3′, *inter-leukin 6 (IL-6)* forward is 5′-GGTACAT CCTCGACGGCATCT-3′ and reverse is 5′-GCCTCTTT GCTGCTTTCAC-3′, *Nod-like receptor protein 3 (NLR P3)* forward is 5′-CTTCTCTGATGAGGCCCAAG-3′ and reverse is 5′- GCAGCAAACTGGAAAGGAAG-3′, *interleukin 24 (IL-24)* forward is 5′-TGTGAAAGA CACTATGCAAGCTC-3′ and reverse is 5′-GTGACA CGATGAGAACAAAGTTG-3′, *Interleukin 6 Family Cytokine (LIF)* forward is 5′-CCAACGTGACGGACT TCCC-3′ and reverse is 5′-TACACGACTATGCGGTA CAGC-3′, and *PIR* forward is 5′-GAGCAGTCGGAAG GGGTTG-3′ and reverse is 5′-TTAACTCGGGTCTGC CAATGC-3′.

Western-blot analysis

Western blot analysis was performed with primary anti-PIR antibody (GeneTex, Irvine, CA, USA), anti-NLRP3 antibody (GeneTex, Irvine, CA, USA), anti-SREBP1

antibody (GeneTex, Irvine, CA, USA), anti-IL-6 antibody (Abcam, Cambridge, MA, USA), anti-IL-1β antibody (GeneTex, Irvine, CA, USA), anti-SIRT1 antibody (Proteintech®, Rosemont, USA), and anti-β-actin antibody (Sigma-Aldrich, St. Louis, MO, USA). The bands corresponding to western blot were quantified using ImageJ.

RNA microarray analysis

Total RNA was corresponding extracted and purified from HPF samples via RNeasy Mini kit (Qiagen®, Valencia, CA, USA) as the initial material and then qualified by Agilent model 2100 Bioanalyzer (Agilent Technologies, Palo Alto, CA, USA). All RNA samples were labeled with the GeneChip 3′IVT Express Kit (Affymetrix, Santa Clara, CA, USA), hybridized, washed, and scanned to the arrays with GeneAtlas Hybridization, Wash, and Stain Kit (Affymetrix, Santa Clara, CA, USA), as described by the manufacturer. Normalization genes were identically represented on the GeneChip Human Genome U133 Plus 2.0 Array (Affymetrix, Santa Clara, CA, USA). Expression of genes was then generated after log2 transformation and normalization with GeneSpring software (Agilent Technologies, Palo Alto, CA, USA). To uncover the significance of genes for further analysis, cutoff values for gene expression results greater than ± 1.5-fold-change were further overlaid onto Ingenuity Pathway Analysis (IPA; QIAGEN, Valencia, CA, USA) to estimate canonical pathways, downstream effects, and potential upstream regulators in response to PM.

In vivo model

6-8-week-old nonobese diabetic/severe combined immunodeficient gamma (NOD.Cg-*Prkdc^{scid} Il2rg^{tm1Wjl}*/SzJ, NOD-SCID γ, NSG™, JAX®, Harbor, ME, USA) male mice (20-25 g body weight) and B6.Cg-*Lep* ^{ob}/J (B6 ob JAX®, Harbor, ME, USA) were used. To establish *in vivo* PM model, PM particles were diluted with 10 µl of PBS and then intratracheally administered into the pulmonary regions with Hamilton syringe. Body weight and behavior were monitored weekly.

Immunohistochemistry staining analysis

Briefly, tissue sections (5 µm) were dewaxed and rehydrated. The slides were incubated in 10 mmol/L citric buffer (pH 6.0). Antigen retrieval was done in Tris-EDTA buffer (pH 9.0) and microwaved for 15 minutes. Endogenous peroxidase activity was blocked by placing the sections in a methanol bath containing 0.5% H$_2$O$_2$. After blocking as above, the slides were incubated with primary antibody against target proteins,

followed by biotin-conjugated secondary antibody polymer-HRP reagent. The endogenous peroxidase activity was then visualized with diaminobenzidine tetrahydroxychloride (DAB) solution.

Public database

Analysis of Gene Expression Omnibus (GEO), a public cohort microarray database, was used to validate the correlation between expression of biomarkers and PM. The differentially expressed genes in the dataset were determined by nonparametric analysis and *t*-test.

Statistical analysis

Statistics analysis was performed with SPSS 17.0 software for Windows (SPSS, Chicago, USA). $P < 0.05$ on a two-sided test was considered significant.

Ethics approval

Animal care and experiments were performed in compliance with 3R principles and approved by the Academia Sinica Institutional Animal Care and Utilization Committee (IACUC).

AUTHOR CONTRIBUTIONS

The study was designed by C-PT, under the direction of MH, Y-CC, and S-CH. The analyses and experiments were performed by C-PT and Y-CC, under examination of C-HC, W-YL, C-SL, K-JL, MH, and S-CH. The manuscript was written by C-PT, C-HC, C-SL, MH, Y-CC and S-CH. The histopathology was analyzed by MH and Y-CC. MH and S-CH provided the reagents and compounds. All authors read and approved the final manuscript.

ACKNOWLEDGMENTS

CONFLICTS OF INTEREST

The authors have no conflicts of interest to declare.

FUNDING

REFERENCES

1. Ambient (outdoor) air quality and health: World Health Organization. 2018. https://www.who.int/news-room/fact-sheets/detail/ambient-(outdoor)-air-quality-and-health

2. Kampa M, Castanas E. Human health effects of air pollution. Environ Pollut. 2008; 151:362–67. https://doi.org/10.1016/j.envpol.2007.06.012 PMID:17646040

3. Pope CA 3rd, Dockery DW. Health effects of fine particulate air pollution: lines that connect. J Air Waste Manag Assoc. 2006; 56:709–42. https://doi.org/10.1080/10473289.2006.10464485 PMID:16805397

4. 9 out of 10 people worldwide breathe polluted air: World Health Organization. 2018. http://www.emro.who.int/media/news/9-out-of-10-people-worldwide-breathe-polluted-air.html

5. Over half a million premature deaths annually in the European Region attributable to household and ambient air pollution.: World Health Organization. 2018. http://www.euro.who.int/en/health-topics/environment-and-health/air-quality/news/news/2018/5/over-half-a-million-premature-deaths-annually-in-the-european-region-attributable-to-household-and-ambient-air-pollution

6. Schauer JJ, Cass GR. Source Apportionment of Wintertime Gas-Phase and Particle-Phase Air Pollutants Using Organic Compounds as Tracers. Environ Sci Technol. 2000; 34:1821–32. https://doi.org/10.1021/es981312t

7. Lodovici M, Bigagli E. Oxidative stress and air pollution exposure. J Toxicol. 2011; 2011:487074. https://doi.org/10.1155/2011/487074 PMID:21860622

8. dos Santos G, Kutuzov MA, Ridge KM. The inflammasome in lung diseases. Am J Physiol Lung Cell Mol Physiol. 2012; 303:L627–33. https://doi.org/10.1152/ajplung.00225.2012 PMID:22904168

9. Jeffery PK. Remodeling in asthma and chronic obstructive lung disease. Am J Respir Crit Care Med. 2001 (supplement_2); 164:S28–38. https://doi.org/10.1164/ajrccm.164.supplement_2.2106061 PMID:11734464

10. Zhang Y, Zheng L, Tuo J, Liu Q, Zhang X, Xu Z, Liu S, Sui G. Analysis of PM$_{2.5}$-induced cytotoxicity in human HaCaT cells based on a microfluidic system. Toxicol In Vitro. 2017; 43:1–8.

https://doi.org/10.1016/j.tiv.2017.04.018
PMID:28431925

11. Zhou L, Su X, Li B, Chu C, Sun H, Zhang N, Han B, Li C, Zou B, Niu Y, Zhang R. PM2.5 exposure impairs sperm quality through testicular damage dependent on NALP3 inflammasome and miR-183/96/182 cluster targeting FOXO1 in mouse. Ecotoxicol Environ Saf. 2019; 169:551–63.
https://doi.org/10.1016/j.ecoenv.2018.10.108
PMID:30476817

12. Calderón-Garcidueñas L, Kavanaugh M, Block M, D'Angiulli A, Delgado-Chávez R, Torres-Jardón R, González-Maciel A, Reynoso-Robles R, Osnaya N, Villarreal-Calderon R, Guo R, Hua Z, Zhu H, et al. Neuroinflammation, hyperphosphorylated tau, diffuse amyloid plaques, and down-regulation of the cellular prion protein in air pollution exposed children and young adults. J Alzheimers Dis. 2012; 28:93–107.
https://doi.org/10.3233/JAD-2011-110722
PMID:21955814

13. Villarreal-Calderon R, Dale G, Delgado-Chávez R, Torres-Jardón R, Zhu H, Herritt L, Gónzalez-Maciel A, Reynoso-Robles R, Yuan Y, Wang J, Solorio-López E, Medina-Cortina H, Calderón-Garcidueñas L. Intra-city Differences in Cardiac Expression of Inflammatory Genes and Inflammasomes in Young Urbanites: A Pilot Study. J Toxicol Pathol. 2012; 25:163–73.
https://doi.org/10.1293/tox.25.163
PMID:22907983

14. Guarnieri M, Balmes JR. Outdoor air pollution and asthma. Lancet. 2014; 383:1581–92.
https://doi.org/10.1016/S0140-6736(14)60617-6
PMID:24792855

15. 2019 GLOBAL STRATEGY FOR PREVENTION, DIAGNOSIS AND MANAGEMENT OF COPD: Global Initiative for Chronic Obstructive Lung Disease (GOLD). 2018.
https://goldcopd.org/wp-content/uploads/2018/11/GOLD-2019-v1.7-FINAL-14Nov2018-WMS.pdf

16. Chronic obstructive pulmonary disease (COPD): World Health Organization. 2017.
https://www.who.int/respiratory/copd/en/

17. Li Y, Xu S, Jiang B, Cohen RA, Zang M. Activation of sterol regulatory element binding protein and NLRP3 inflammasome in atherosclerotic lesion development in diabetic pigs. PLoS One. 2013; 8:e67532.
https://doi.org/10.1371/journal.pone.0067532
PMID:23825667

18. Horton JD, Goldstein JL, Brown MS. SREBPs: activators of the complete program of cholesterol and fatty acid synthesis in the liver. J Clin Invest.

2002; 109:1125–31.
https://doi.org/10.1172/JCI0215593 PMID:11994399

19. Ponugoti B, Kim DH, Xiao Z, Smith Z, Miao J, Zang M, Wu SY, Chiang CM, Veenstra TD, Kemper JK. SIRT1 deacetylates and inhibits SREBP-1C activity in regulation of hepatic lipid metabolism. J Biol Chem. 2010; 285:33959–70.
https://doi.org/10.1074/jbc.M110.122978
PMID:20817729

20. Licciulli S, Luise C, Zanardi A, Giorgetti L, Viale G, Lanfrancone L, Carbone R, Alcalay M. Pirin delocalization in melanoma progression identified by high content immuno-detection based approaches. BMC Cell Biol. 2010; 11:5.
https://doi.org/10.1186/1471-2121-11-5
PMID:20089166

21. Solomon JM, Pasupuleti R, Xu L, McDonagh T, Curtis R, DiStefano PS, Huber LJ. Inhibition of SIRT1 catalytic activity increases p53 acetylation but does not alter cell survival following DNA damage. Mol Cell Biol. 2006; 26:28–38.
https://doi.org/10.1128/MCB.26.1.28-38.2006
PMID:16354677

22. Hawkins JL, Robbins MD, Warren LC, Xia D, Petras SF, Valentine JJ, Varghese AH, Wang IK, Subashi TA, Shelly LD, Hay BA, Landschulz KT, Geoghegan KF, Harwood HJ Jr. Pharmacologic inhibition of site 1 protease activity inhibits sterol regulatory element-binding protein processing and reduces lipogenic enzyme gene expression and lipid synthesis in cultured cells and experimental animals. J Pharmacol Exp Ther. 2008; 326:801–08.
https://doi.org/10.1124/jpet.108.139626
PMID:18577702

23. Miyazaki I, Simizu S, Okumura H, Takagi S, Osada H. A small-molecule inhibitor shows that pirin regulates migration of melanoma cells. Nat Chem Biol. 2010; 6:667–73. https://doi.org/10.1038/nchembio.423
PMID:20711196

24. Quay JL, Reed W, Samet J, Devlin RB. Air pollution particles induce IL-6 gene expression in human airway epithelial cells via NF-kappaB activation. Am J Respir Cell Mol Biol. 1998; 19:98–106.
https://doi.org/10.1165/ajrcmb.19.1.3132
PMID:9651185

25. Ljungman P, Bellander T, Schneider A, Breitner S, Forastiere F, Hampel R, Illig T, Jacquemin B, Katsouyanni K, von Klot S, Koenig W, Lanki T, Nyberg F, et al. Modification of the interleukin-6 response to air pollution by interleukin-6 and fibrinogen polymorphisms. Environ Health Perspect. 2009; 117:1373–79.
https://doi.org/10.1289/ehp.0800370

PMID:19750100

26. Valavanidis A, Vlachogianni T, Fiotakis K, Loridas S. Pulmonary oxidative stress, inflammation and cancer: respirable particulate matter, fibrous dusts and ozone as major causes of lung carcinogenesis through reactive oxygen species mechanisms. Int J Environ Res Public Health. 2013; 10:3886–907. https://doi.org/10.3390/ijerph10093886 PMID:23985773

27. Wendler WM, Kremmer E, Förster R, Winnacker EL. Identification of pirin, a novel highly conserved nuclear protein. J Biol Chem. 1997; 272:8482–89. https://doi.org/10.1074/jbc.272.13.8482 PMID:9079676

28. Gelbman BD, Heguy A, O'Connor TP, Zabner J, Crystal RG. Upregulation of pirin expression by chronic cigarette smoking is associated with bronchial epithelial cell apoptosis. Respir Res. 2007; 8:10. https://doi.org/10.1186/1465-9921-8-10 PMID:17288615

29. Licciulli S, Cambiaghi V, Scafetta G, Gruszka AM, Alcalay M. Pirin downregulation is a feature of AML and leads to impairment of terminal myeloid differentiation. Leukemia. 2010; 24:429–37. https://doi.org/10.1038/leu.2009.247 PMID:20010624

30. Mercer BA, Lemaître V, Powell CA, D'Armiento J. The Epithelial Cell in Lung Health and Emphysema Pathogenesis. Curr Respir Med Rev. 2006; 2:101–42. https://doi.org/10.2174/157339806776843085 PMID:19662102

31. Harvey BG, Heguy A, Leopold PL, Carolan BJ, Ferris B, Crystal RG. Modification of gene expression of the small airway epithelium in response to cigarette smoking. J Mol Med (Berl). 2007; 85:39–53. https://doi.org/10.1007/s00109-006-0103-z PMID:17115125

32. Rastrick JM, Stevenson CS, Eltom S, Grace M, Davies M, Kilty I, Evans SM, Pasparakis M, Catley MC, Lawrence T, Adcock IM, Belvisi MG, Birrell MA. Cigarette smoke induced airway inflammation is independent of NF-κB signalling. PLoS One. 2013; 8:e54128. https://doi.org/10.1371/journal.pone.0054128 PMID:23349803

33. Cho HY, Wang X, Li J, Bell DA, Kleeberger SR. Potential therapeutic targets in Nrf2-dependent protection against neonatal respiratory distress disease predicted by cDNA microarray analysis and bioinformatics tools. Curr Opin Toxicol. 2016; 1:125–33. https://doi.org/10.1016/j.cotox.2016.10.006 PMID:28920101

34. Legutko A, Marichal T, Fiévez L, Bedoret D, Mayer A, de Vries H, Klotz L, Drion PV, Heirman C, Cataldo D, Louis R, Thielemans K, Andris F, et al. Sirtuin 1 promotes Th2 responses and airway allergy by repressing peroxisome proliferator-activated receptor-γ activity in dendritic cells. J Immunol. 2011; 187:4517–29. https://doi.org/10.4049/jimmunol.1101493 PMID:21948987

35. Wu Z, Liu MC, Liang M, Fu J. Sirt1 protects against thrombomodulin down-regulation and lung coagulation after particulate matter exposure. Blood. 2012; 119:2422–29. https://doi.org/10.1182/blood-2011-04-350413 PMID:22262770

36. Zhang HN, Li L, Gao P, Chen HZ, Zhang R, Wei YS, Liu DP, Liang CC. Involvement of the p65/RelA subunit of NF-kappaB in TNF-alpha-induced SIRT1 expression in vascular smooth muscle cells. Biochem Biophys Res Commun. 2010; 397:569–75. https://doi.org/10.1016/j.bbrc.2010.05.160 PMID:20617556

37. D'Onofrio N, Servillo L, Balestrieri ML. SIRT1 and SIRT6 Signaling Pathways in Cardiovascular Disease Protection. Antioxid Redox Signal. 2018; 28:711–32. https://doi.org/10.1089/ars.2017.7178 PMID:28661724

38. You M, Cao Q, Liang X, Ajmo JM, Ness GC. Mammalian sirtuin 1 is involved in the protective action of dietary saturated fat against alcoholic fatty liver in mice. J Nutr. 2008; 138:497–501. https://doi.org/10.1093/jn/138.3.497 PMID:18287356

39. Liu GZ, Hou TT, Yuan Y, Hang PZ, Zhao JJ, Sun L, Zhao GQ, Zhao J, Dong JM, Wang XB, Shi H, Liu YW, Zhou JH, et al. Fenofibrate inhibits atrial metabolic remodelling in atrial fibrillation through PPAR-α/sirtuin 1/PGC-1α pathway. Br J Pharmacol. 2016; 173:1095–109. https://doi.org/10.1111/bph.13438 PMID:26787506

40. Zhao S, Li J, Wang N, Zheng B, Li T, Gu Q, Xu X, Zheng Z. Fenofibrate suppresses cellular metabolic memory of high glucose in diabetic retinopathy via a sirtuin 1-dependent signalling pathway. Mol Med Rep. 2015; 12:6112–18. https://doi.org/10.3892/mmr.2015.4164 PMID:26238659

41. Wang W, Lin Q, Lin R, Zhang J, Ren F, Zhang J, Ji M, Li Y. PPARα agonist fenofibrate attenuates TNF-α-induced CD40 expression in 3T3-L1 adipocytes via the SIRT1-dependent signaling pathway. Exp Cell Res. 2013; 319:1523–33. https://doi.org/10.1016/j.yexcr.2013.04.007

PMID:23603572

42. Oishi Y, Spann NJ, Link VM, Muse ED, Strid T, Edillor C, Kolar MJ, Matsuzaka T, Hayakawa S, Tao J, Kaikkonen MU, Carlin AF, Lam MT, et al. SREBP1 Contributes to Resolution of Pro-inflammatory TLR4 Signaling by Reprogramming Fatty Acid Metabolism. Cell Metab. 2017; 25:412–27.
https://doi.org/10.1016/j.cmet.2016.11.009
PMID:28041958

43. Lozano R, Naghavi M, Foreman K, Lim S, Shibuya K, Aboyans V, Abraham J, Adair T, Aggarwal R, Ahn SY, Alvarado M, Anderson HR, Anderson LM, et al. Global and regional mortality from 235 causes of death for 20 age groups in 1990 and 2010: a systematic analysis for the Global Burden of Disease Study 2010. Lancet. 2012; 380:2095–128.
https://doi.org/10.1016/S0140-6736(12)61728-0
PMID:23245604

44. Barnes PJ. Inflammatory mechanisms in patients with chronic obstructive pulmonary disease. J Allergy Clin Immunol. 2016; 138:16–27.
https://doi.org/10.1016/j.jaci.2016.05.011
PMID:27373322

45. Shaw JG, Vaughan A, Dent AG, O'Hare PE, Goh F, Bowman RV, Fong KM, Yang IA. Biomarkers of progression of chronic obstructive pulmonary disease (COPD). J Thorac Dis. 2014; 6:1532–47.
https://doi.org/10.3978/j.issn.2072-1439.2014.11.3
PMID:25478195

46. Sin DD, Vestbo J. Biomarkers in chronic obstructive pulmonary disease. Proc Am Thorac Soc. 2009; 6:543–45.
https://doi.org/10.1513/pats.200904-019DS
PMID:19741266

47. Lock-Johansson S, Vestbo J, Sorensen GL. Surfactant protein D, Club cell protein 16, Pulmonary and activation-regulated chemokine, C-reactive protein, and Fibrinogen biomarker variation in chronic obstructive lung disease. Respir Res. 2014; 15:147.
https://doi.org/10.1186/s12931-014-0147-5
PMID:25425298

48. Dickens JA, Miller BE, Edwards LD, Silverman EK, Lomas DA, Tal-Singer R, and Evaluation of COPD Longitudinally to Identify Surrogate Endpoints (ECLIPSE) study investigators. COPD association and repeatability of blood biomarkers in the ECLIPSE cohort. Respir Res. 2011; 12:146.
https://doi.org/10.1186/1465-9921-12-146
PMID:22054035

49. Ilumets H, Rytilä P, Demedts I, Brusselle GG, Sovijärvi A, Myllärniemi M, Sorsa T, Kinnula VL. Matrix metalloproteinases -8, -9 and -12 in smokers and patients with stage 0 COPD. Int J Chron Obstruct Pulmon Dis. 2007; 2:369–79.
https://doi.org/10.1186/1465-9921-7-69
PMID:18229576

50. Culpitt SV, Maziak W, Loukidis S, Nightingale JA, Matthews JL, Barnes PJ. Effect of high dose inhaled steroid on cells, cytokines, and proteases in induced sputum in chronic obstructive pulmonary disease. Am J Respir Crit Care Med. 1999; 160:1635–39.
https://doi.org/10.1164/ajrccm.160.5.9811058
PMID:10556133

51. Sng JJ, Prazakova S, Thomas PS, Herbert C. MMP-8, MMP-9 and Neutrophil Elastase in Peripheral Blood and Exhaled Breath Condensate in COPD. COPD. 2017; 14:238–44.
https://doi.org/10.1080/15412555.2016.1249790
PMID:27880043

52. Ichikawa T, Hayashi R, Suzuki K, Imanishi S, Kambara K, Okazawa S, Inomata M, Yamada T, Yamazaki Y, Koshimizu Y, Miwa T, Matsui S, Usui I, et al. Sirtuin 1 activator SRT1720 suppresses inflammation in an ovalbumin-induced mouse model of asthma. Respirology. 2013; 18:332–39.
https://doi.org/10.1111/j.1440-1843.2012.02284.x
PMID:23062010

53. Deng F, Guo X, Liu H, Fang X, Yang M, Chen W. Effects of dust storm PM2.5 on cell proliferation and cell cycle in human lung fibroblasts. Toxicol In Vitro. 2007; 21:632–38.
https://doi.org/10.1016/j.tiv.2006.12.013
PMID:17306959

SUPPLEMENTARY MATERIALS
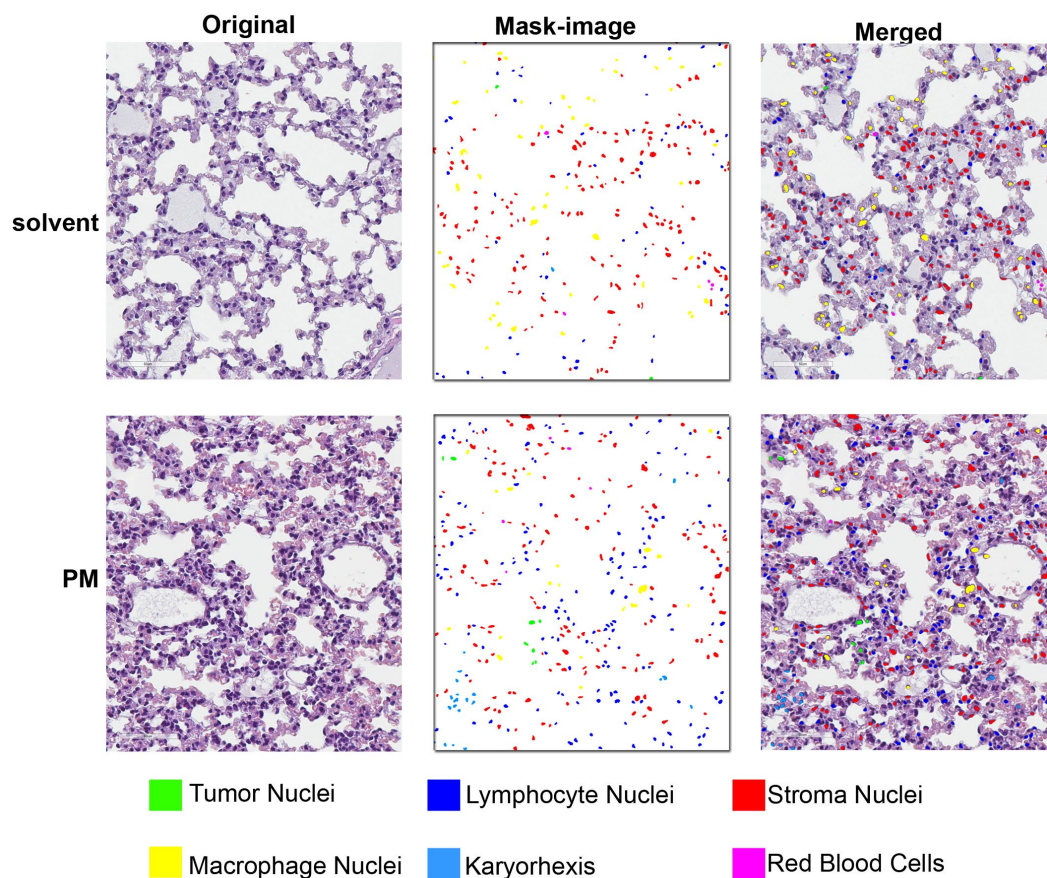
Supplementary Figure 1. PM induces adverse health events via multi-factorial mechanisms: Utilized Hematoxylin/Eosin staining of mice lung through Mask-RCNN based pathology image training model combined with deep-learning algorithm, PM-fed groups recruit more lymphocytes (blue) and stroma cell (red) than solvent control.
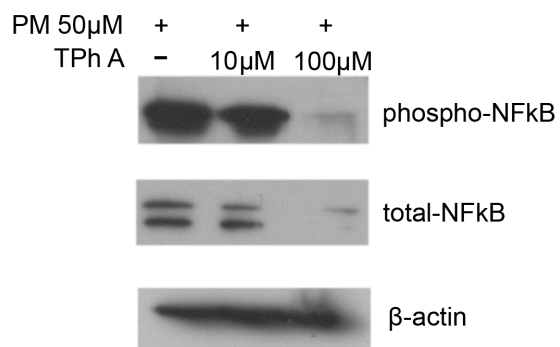
Supplementary Figure 2. NF-κB is negtively correlated with TPh A. Western blot analysis of phosphor-NFκB and total-NFκB in TPh A-PM co-treated HPF models.

Please browse Full Text version to see the data of Supplementary Table:
Supplementary Table 1. HPF 1.5 cut-off.